European Journal of
Nuclear
Medicine

Original article

Principal component analysis of dynamic positron emission tomography images

F. Pedersen[1], M. Bergström[2], E. Bengtsson[1], B. Långström[2]

[1] Centre for Image Analysis, Uppsala University, Uppsala, Sweden
[2] PET Center, Uppsala University, University Hospital, Uppsala, Sweden

Received 15 April and in revised form 30 June 1994

Abstract. Multivariate image analysis can be used to analyse multivariate medical images. The purpose could be to visualize or classify structures in the image. One common multivariate image analysis technique which can be used for visualization purposes is principal component analysis (PCA). The present work concerns visualization of organs and structures with different kinetics in a dynamic sequence utilizing PCA. When applying PCA on positron emission tomography (PET) images, the result is initially not satisfactory. It is illustrated that one major explanation for the behaviour of PCA when applied to PET images is that it is a data-driven technique which cannot separate signals from high noise levels. With a better understanding of the PCA, gained with a strategy of examining the image data set, the transformations, and the results using visualization tools, a surprisingly easily understood methodology can be derived. The proposed methodology can enhance clinically interesting information in a dynamic PET imaging sequence in the first few principal component images and thus should be able to aid in the identification of structures for further analysis.

Key words: PET imaging – Multivariate image analysis – Principal component analysis – Visualization of multidimensional data

Eur J Nucl Med (1994) 21:1285–1292

Introduction

Multivariate statistical methods are used for classification [1], regression [2] and factor analysis (FA) [3]. These multivariate statistical methods have been used over two decades for different purposes in the analysis of multispectral images in the remote sensing discipline [4]. Some multivariate methods have also been used in medical imaging for quite some time [5].

A collection of approaches, including multivariate statistical methods for tissue characterization in magnetic resonance (MR) imaging, are presented in [6]. In nuclear medicine [positron emission tomography (PET), gamma camera imaging], the multivariate analysis of image data is mostly concerned with estimating the parameters of a compartment model [7]. The methodology is referred to as factor analysis of dynamic structures (FADS). In [8] several proposals for performing FADS are reviewed. It is well known that FADS is used to solve an under-determined problem. There are an infinite number of sets of factors which are possible solutions. The modifications done to the original algorithms mainly propose different constraints on the solution in order to reduce the set of possible factors.

A starting point for the multivariate statistical methods could be a principal component analysis (PCA) [9–11]. PCA is a data-driven technique used to explain the variance-covariance structure in a data set through a set of linear combinations of the original variables. PCA is often used to find a first set of factors in a factor analysis. In [12], one of the pioneers in the area reviews the use of FA in nuclear medicine. It is pointed out that FA is used to overcome some of the limitations of a region of interest (ROI) analysis, but FA introduces new problems, such as interpretation of the obtained factors. FA could, however, be incorporated in the ROI analysis instead of being an alternative. It is suggested that FA could have a role in improving reproducibility in the ROI analysis. This paper is concerned with this matter. We will re-examine the possibility of using the conceptually simple PCA on dynamic imaging sequences for visualizing in a few images the major structures in the sequence. This approach can be used as an intermediate step in an ROI analysis.

Correspondence to: F. Pedersen, Centre for Image Analysis, Uppsala University, Lägerhyddvägen 17, S-752 37 Uppsala, Sweden

Materials and methods

A short description of multivariate images and PCA is presented in Appendix **A**.

Synthetic image data. In order to understand the result of applying PCA on multivariate images, synthetic images simulating simple but representative dynamics are used. Two synthetic multivariate images with a spatial size of 128×128 pixels, and with grey scale in the range 0–4095 (12 bit pixels), will be used.

The first synthetic multivariate image consists of two images. It contains background, two circular homogeneous areas with changing grey levels, and additive noise. The standard deviation is fixed for each image, so all signals in an image have the same noise. The signals were designed to be linearly related, which gives a true dimensionality of one. This multivariate data set is described by three normal distributions and the number of samples from the corresponding normal distribution (Table 1).

The second synthetic multivariate image consists of ten images. It contains a constant background and three small circular homogeneous areas with grey levels changing for the different bands, as defined in Table 2.

PET image data. Four different PET image data sets utilizing different tracers will be used as illustrations. The images all have a spatial size of 128×128 pixels. The grey scale is in the range 0–4095. The number of collected frames varies between 10 and 20 for the different acquisitions.

Background noise normalization. The synthetic multivariate image defined in Table 1, shown in Figure 1a, simulates two images from the same slice but different frames in a dynamic PET imaging sequence. The important properties are different background noise, and two structures which are close in amplitude. For a more detailed discussion of the proposed background noise normalization than is presented in this section, see [13] and [14].

Performing PCA of this multivariate image results in a new, transformed, multivariate image. The images contained in this new multivariate image, the principal component (PC) images, represents orthogonal maximum variance directions for the analysed data set. Mathematically, these directions are derived as the eigenvectors of the covariance matrix for the data set. PCA is a data-driven technique, which cannot by itself discriminate between signals and noise. In this section we would like to illustrate how the background noise can influence the choices of the maximum variance directions.

The space spanned by a p-dimensional histogram of the p image bands in a multivariate image will be called feature space. It is in this space that the PCA selects the maximum variance directions. A visualization of this space is the 2D histogram, often re-

Table 1. Definition of the signals in a noisy synthetic multivariate image with two dimensions. The used notation for the normal distribution is $N(m_{ij}, \sigma_i)$. m_{ij} is the mean value for the signal j in image band i; σ_i is the standard deviation for all signals in image band i. n_j samples are present from the signal j in all bands. The corresponding images are shown in Fig. 1 a

Image band i (variable)	$S1_{1i}$ (big object) $n_1 \approx 530$	$S1_{2i}$ (medium object) $n_2 \approx 200$	$S1_{3i}$ (background) $n_3 \approx 15\,650$
1	N (2300, 300)	N (2600, 300)	N (2000, 300)
2	N (2200, 50)	N (2400, 50)	N (2000, 50)

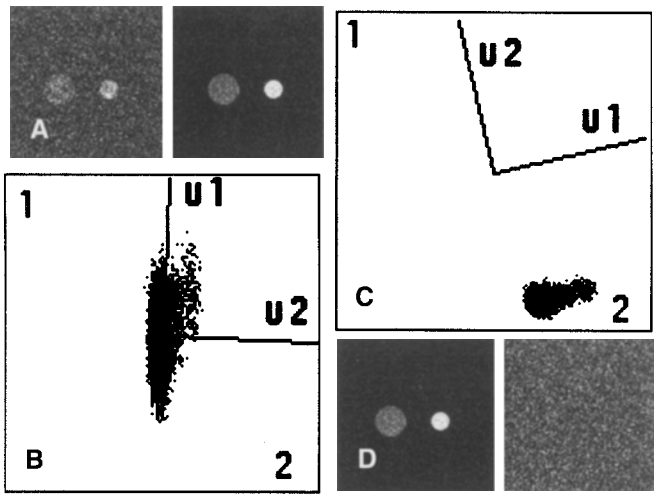

Fig. 1. a The two images bands defined by Table 1. The first band is to the *left*, the second is to the *right*. The visible signals are the big object $S1_1$, the medium object $S1_2$, and the background $S1_3$. Note that the two bands have different noise. **b** The feature space for the first synthetic image represented as a scatter plot. The eigenvectors $\mathbf{u}_1$ and $\mathbf{u}_2$ obtained from the PCA are indicated. This type of plot will be called an eigenvector-scatter plot. **c** The eigenvector-scatter plot for the case of using noise normalized image data. Note how the shape of the clusters in feature space have changed from elliptical to circular, and that the first eigenvector points out a direction given by the centres of gravity for the clusters. **d** The result of a PCA of the noise-normalized synthetic multivariate image. PC1 to the *left*, PC2 to the *right*. The structures are only visible in PC1

Table 2. Three signals and a background defined for a ten-dimensional synthetic multivariate image. The signals are plotted in Fig. 2a, and the images are shown in Fig. 2b

Image band (variable)	$S2_{1i}$ (big object) $n_1 \approx 530$	$S2_{2i}$ (medium object) $n_2 \approx 200$	$S2_{3i}$ (small object) $n_3 \approx 110$	$S2_{4i}$ (background) $n_4 \approx 15\,540$
$i = 1..10$	$3000 \exp(0.5i) - 4000 (1 - \exp(0.06i))$	$3000 \exp(0.07i)$	$3000 (1 - \exp(0.22i)$	100

ferred to as a scatter plot. For image data, it shows the position of the pixels in a 2D subspace of feature space. If the multivariate image consists of only two images, the scatter plot shows the whole feature space. The feature space for the example image is shown in Fig. 1b. The numbers in the plot indicate which axis represents which image.

A scatter plot with indicated eigenvectors will be referred to as an eigenvector-scatter plot. Figure 1b is an eigenvector-scatter plot. The eigenvectors $\mathbf{u}_1$ and $\mathbf{u}_2$ are shown in the plot; note that they are orthogonal. It is possible to examine the characteristics of the PC images using the eigenvector-scatter plot.

The unequal background noise in the two images in the used synthetic multivariate image is visible in the feature space representation as producing elliptically shaped signals. The first eigenvector $\mathbf{u}_1$ does not indicate the two structures, but points out a direction very much influenced by the large background noise in the first image, which in the figure is vertically directed. The two resulting PC images will be very similar to the two original images (see Fig. 1a).

All parameters, including the noise, are known for this synthetic data set. It is then possible to normalize the data to uniform noise. The result will be circular blobs in feature space, and three overlapping circular blobs representing the three signals are visible in Fig. 1c. After the background noise normalization, the two structures are successfully indicated by the first eigenvector because the centres of gravity for the circular blobs representing the signals now define the maximum variance direction. The structures will in this case be shown in good contrast in the corresponding image PC1 (Fig. 1d).

From this example with noisy synthetic data an important conclusion can be drawn. Preprocessing by normalization of the background noise can improve the possibility to separate signals from noise using PCA, a task which PCA itself is not capable of solving since it is data driven. The method is motivated from numerical experiments [13], and has theoretical support [15].

Results

PCA of a noise-free synthetic image

The values for the different signals in the noise-free synthetic multivariate image are plotted in Fig. 2a. The synthetic image, shown in Fig. 2b, is subject to a PCA. In Fig. 2c the first five obtained PC images are shown. Higher PC images are similar to PC4 and PC5, containing no structure. As expected, there is a substantial reduction in the dimensionality. Only the first three PC images contain structure. It is possible to give a simple interpretation of these PC images by observing the weights of the corresponding eigenvectors, but this is beyond the scope of this paper. This synthetic image data set has only three dimensions, even though ten dimensions are initially used to describe the data set. This performance of PCA, creating PC images showing the signals contrasted to one another, is believed to be useful as a preprocessing step before an ROI analysis.

A methodology for applying PCA to PET image data sets

Figure 3a shows the same slice imaged in ten frames in a dynamic PET head scan. It is a study of the brain in a patient with temporal lobe epilepsy using the tracer ^{11}C-L-deuterium-deprenyl. In the sequence of image bands there are early, late and more complex signals. The result from the previous section suggests that improved contrasts between the different signals should be obtained through a PCA. In Fig. 3b the result of a PCA is shown. The behaviour is not as expected. The major signal components are not contrasted in the first few PC images; instead signals appear in many of the PC images.

The PCA has failed to reproduce the result obtained in the previous section using the noise-free synthetic im-

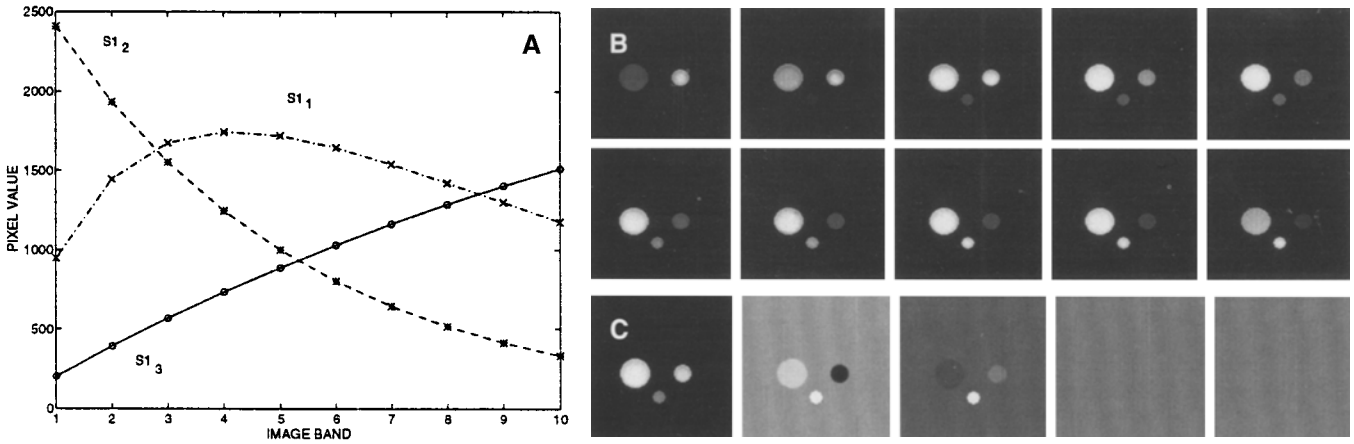

Fig. 2. **a** Time-activity curves for the three signals defined in Table 2, shown in Fig. 2b. **b** The ten image bands defined by Table 2. The first band is in the *upper left corner*, and the tenth band is in the *lower right corner*. This set up will be used for all images, and the images are always shown contrast stretched. **c** The first five PC images obtained when PCA is applied to the noise-free synthetic image shown in **b**. From *left* to *right*: PC1 to PC5. The dimensionality is reduced to three

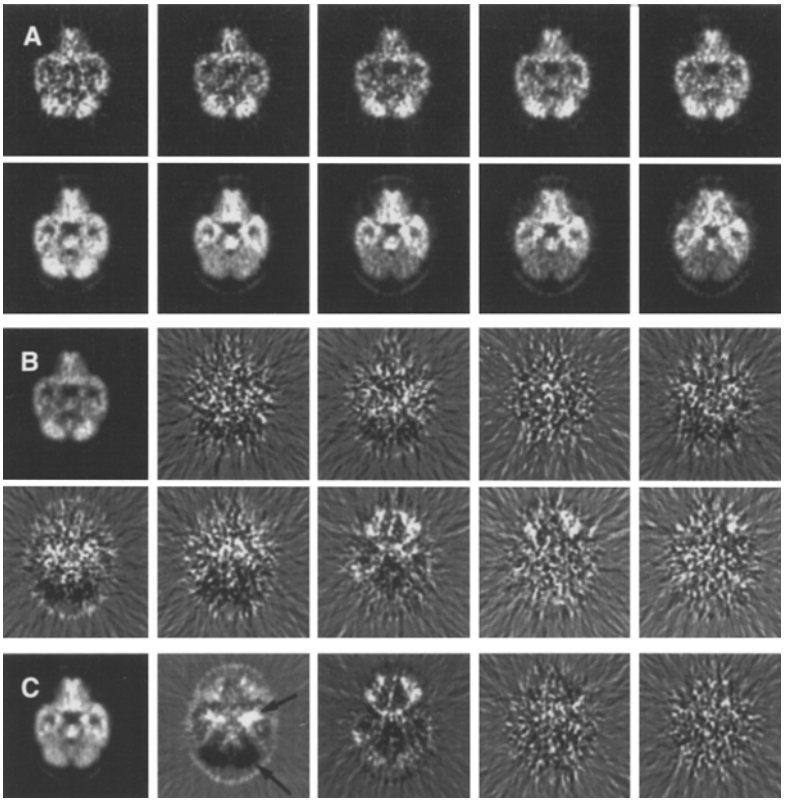

Fig. 3. a One slice from a dynamic study of the brain in a patient with temporal lobe epilepsy using the tracer ^{11}C-L-deuterium-deprenyl. **b** The ten PC images derived through a PCA of the PET image in **a**. Structures are visible in many of the PC images. **c** The first five PC images obtained after noise normalization and PCA of the PET image shown in **a**. In PC2, the epileptic focus (*bright area*) and the cerebellum (*dark area*) are indicated

age data. Since PCA is a data-driven technique, the explanation of the difference in the result from the synthetic and the real image data is not to be found in the mode of analysis, but in the properties of the data set.

A multivariate image contains information which can be hard to fully comprehend due to the high dimensionality of the data set. The work presented in this paper was carried out using a software called MUSE [16], designed for exploratory interactive multivariate image analysis [17, 18]. Using MUSE, real and synthetic image data, the influence of background noise was identified as a major factor contributing to the disadvantageous result of PCA when applied on raw PET image data.

In order to compensate for the difference in background noise, one starts by estimating the background noise for each slice and frame. An estimate of the background noise can be obtained using an ROI situated in the background. Alternatively, an estimate of the background noise can be made from the image reconstruction data. The noise in a slice is approximately proportional to the number of counts registered for this particular slice and frame. The noise in the investigated slice is normalized for each frame using the estimate, i.e. the investigated PET image is noise normalized. PCA is applied to this preprocessed image data set.

Applying the proposed methodology, using an automatic estimation of the noise (from the reconstruction data), to the PET example in Fig. 3a results in the PC images shown in Fig. 3c. A visual comparison of the PC images in Fig. 3c to the PC images in Fig. 3b indicates that the signals are better visualized using noise-normalized image data.

The signal-to-noise ratios (SNRs; see Appendix B for a definition) for the two cases are shown in Fig. 4. In order to display the differences for the higher PCs, Fig. 4 does not show the SNRs for the first PC. It is close to 230 for both cases. The plot indicates that the noise is more successfully handled in the case of noise-normalized image data, because when the noise level is reached it is stable. Compare this to the non-normalized case, where there are increases in SNR for higher PC images. Those PC images show structure even though the noise level should have been reached. The plot of the SNRs supports the visual impression that the appearance of the signals is more favourable if the noise normalization is used, and they appear in the first few PC images only. In conclusion, PCA applied to noise-normalized image data will show a result which is more in line with what would be achieved using a noise-free image data set.

Applying PCA to several PET image data sets

Four different PET image data sets utilizing four different tracers will be used to illustrate the potential of performing PCA of automatically noise normalized PET images. The result will be PC images which highlight spatial areas with different kinetic behaviour. Dynamic

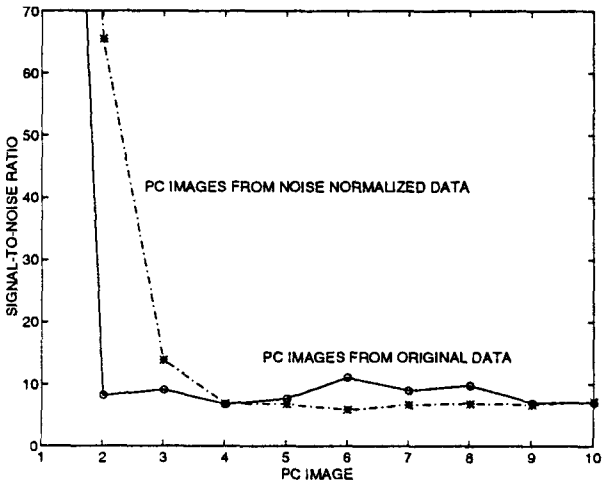

Fig. 4. A plot showing the SNRs for the PC images derived from the original PET data (Fig. 3b) and the PC images derived from the noise-normalized PET data (Fig. 3c)

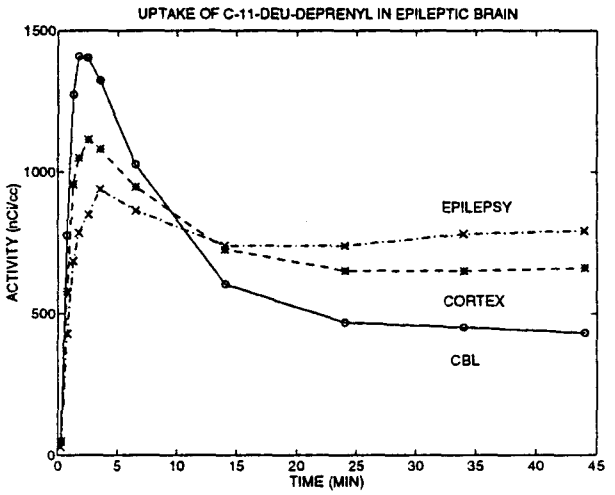

Fig. 5. The dynamic curves plotted for the relevant structures in Fig. 3c

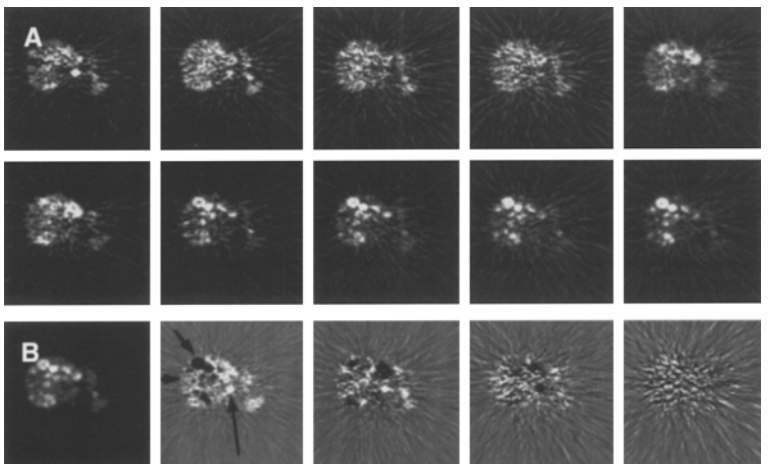

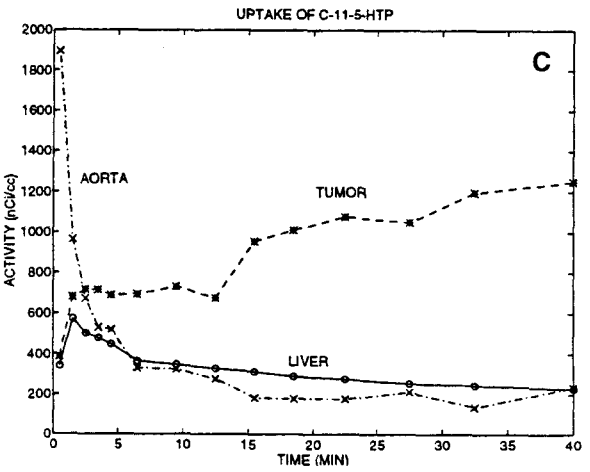

Fig. 6. a A slice through the abdomen, including the liver, in a patient with a multitude of metastases from a carcinoid tumour examined after the injection of ^{11}C-5-hydroxytryptophan. **b** The first five PC images obtained after noise normalization and PCA of the PET image shown in **a**. Indicated structures in PC2 are the aorta (*bright area*), the tumours (*dark area*) and the liver (*grey area*). **c** The dynamic curves plotted for the relevant structures in **b**

curves for these areas are obtained from interactively marked ROIs.

Figure 3c shows the first five PC images for the previously used example with ^{11}C-L-deuterium-deprenyl in a patient with temporal lobe epilepsy. The weighted average image PC1 shows lower uptake in the cerebellum (CBL). From PC2 and the dynamic curves shown in Fig. 5 it is seen that the uptake in the cerebellum differs from cortex and epileptic focus, with a pronounced initial uptake followed by a more significant washout. The epileptic focus is contrasted against normal brain tissue with a low initial uptake and high late uptake.

Figure 6a shows a slice through the abdomen, including the liver, in a patient with a multitude of metastases from a carcinoid tumour. Ten of the used 14 frames are shown. The patient was examined after the injection of ^{11}C-5-hydroxytryptophan, a tracer which indicates the synthesis of serotonin which is extensive in this type of tumour [19]. In the PC images in Fig. 6b, a very high uptake of ^{11}C-5-hytroxytryptophan is nicely demonstrated in PC1. The second PC image indicates not only that the magnitude of the uptake in the tumour metastases is enhanced, but it clearly also demonstrates a different kinetic pattern compared to the liver. The aorta with its separate kinetics is also highlighted. The kinetic curves obtained in ROIs in the liver, the metastases and the aorta are demonstrated in Fig. 6c.

Figure 7a shows a slice through the abdomen in a patient with a large ductal pancreatic tumour and a small metastasis in the tip of the liver obtained with ^{18}F-flu-

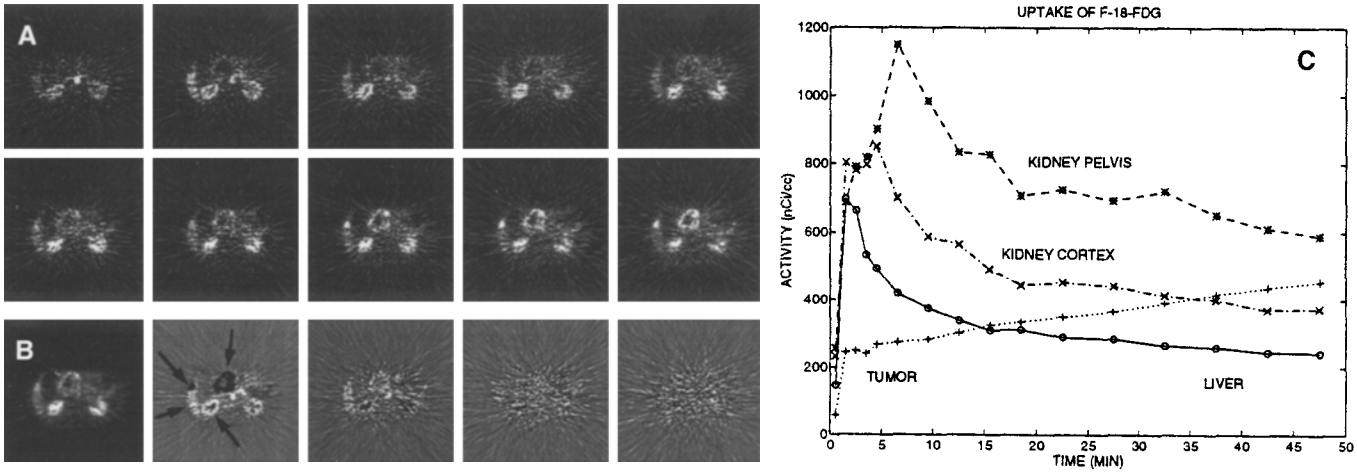

Fig. 7. a A slice through the abdomen in a patient with a large ductal pancreatic tumour and a small metastasis in the tip of the liver obtained with ^{18}F-fluorodeoxyglucose. **b** The first five PC images obtained after noise normalization and PCA of the PET image shown in **a.** Indicated structures in PC2 are tumours (*upper dark areas*), the liver (*bright area to the left*) and a kidney (*bright round structure in the centre*). **c** The dynamic curves plotted for the relevant structures in **b**

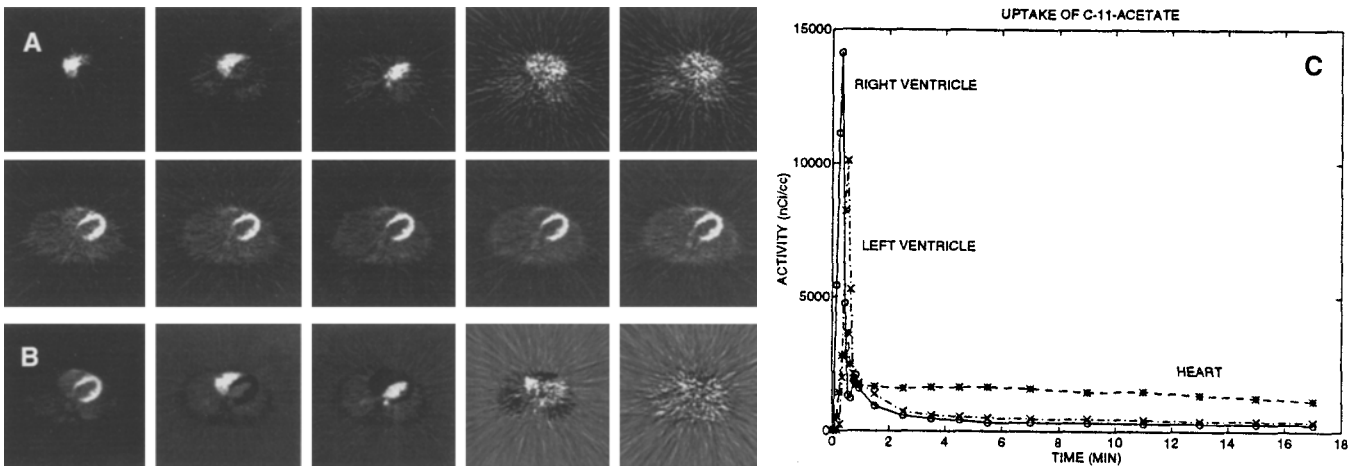

Fig. 8. a A slice through the thoracic region, including the heart and lung, after the injection of ^{11}C-acetate for the visualization of the oxidative metabolism in the heart. **b** The first five PC images obtained after noise normalization and PCA of the PET image shown in **a**. The different kinetics of the ventricles are well captured in PC2 and PC3. **c** The dynamic curves plotted for the relevant structures in **b**

orodeoxyglucose. Figure 7b shows that the magnitude of the uptake of ^{18}F-fluorodeoxyglucose averaged over the sequence is only slightly enhanced in the tumour, as seen in PC1. PC2 shows that the kinetics of the tumours are significantly different from those observed in the liver. The kinetic patterns obtained in ROIs are shown in Fig. 7c.

Figure 8a shows a slice through the thoracic region, including the heart and lung, after the injection of ^{11}C-acetate for the visualization of the oxidative metabolism in the heart. The first PC image in Fig. 8b documents the very high uptake in the heart muscle. The following two PCs separate the time sequences of initial passage of the blood radioactivity into the right ventricle followed by passage into the left ventricle. The kinetic patterns obtained in ROIs are shown in Fig. 8c.

Discussion

Positron emission tomography is undergoing very rapid development, primarily due to the multitude of new tracer substances which are available for human studies. Many of these new tracers necessitate dynamic examinations and dynamic models for analysis which consider the relative contributions from blood volume with a variable blood concentration, organ perfusion, partition coefficients, reversible and irreversible binding, metabo-

lism of the tracer and washout from the organ. The complex dynamic behaviour often makes it difficult to identify anatomical structures which differ in one or more respects. It is logical to assume that inspection of only a few frames in a dynamic sequence or an image obtained as an average over part of the examination, is not sufficient.

In the present communication we propose a methodology, PCA of a dynamic PET study, to aid in the identification of structures with different kinetic patterns. This identification can be used as a starting point for different types of analysis, e.g. kinetic analysis of an ROI placed on the basis of anatomical identification also using PC images. This method can be viewed as a technique to reduce the dimensionality of the data set by successive identification of which components constitute maximum variance, and to illustrate these components as images.

The methodology includes three attractive features. Firstly, the PC images will appear with decreasing SNR (see Fig. 4). Therefore only the first few PC images need to be inspected. Only in cases with higher dimensionality in the dynamic behaviour will structures appear in higher PCs. Secondly, the method is optimizing the signals by simultaneously considering the complete set of images in the dynamic sequence. Thirdly, the method is totally independent of any kinetic model and thus does not include any model-based restrictions.

It is possible to perform local PC transformations (see Appendix **A**) using an ROI which covers the objects. For the presented PET images, using an ROI improves the SNRs for the first few PCs, but without major visual improvement. It is believed that using an ROI improves the behaviour of PCA, but the improvement is too small to be clearly visible. The reason for this belief is that if the pixels belonging to the background are used in the calculations, the direction of the first eigenvector is strongly influenced by those pixels, and this influences the following eigenvectors because of the orthogonality between eigenvectors. An ROI which excludes a large part of the background reduces its influence on the eigenvectors.

It should be noted that the procedure to normalize the background noise in each slice and frame creates frames with equal noise levels for all slices. This is equivalent to expressing all pixels with the same uncertainty.

An implementation of the proposed methodology is currently in use for evaluation at the PET Center, Uppsala University. The implementation uses automatic estimations of the noise, and also has the possibility of using local PC transformations. Using a modern workstation, the calculation of the PC images for all slices takes 5–10 min, depending on the number of frames. The clinical material presented was processed using this software.

Application of PCA to SPET imaging sequences is clearly possible, without any modifications of the methodology. If the methodology is applied to gamma camera data, the noise normalization should be replaced by noise stabilization of the Poisson-distributed noise [14].

In conclusion, a methodology for applying PCA to PET sequence image data has been proposed. It uses an estimate of the background noise in each slice and frame to normalize the images to equal noise level. Application of PCA to these preprocessed PET image data results in PC images with structures of interest visible in only the first few PC images.

Acknowledgements. This work was partially supported by grants from the Swedish Cancer Society. The clinical images were kindly supplied by Dr. Sven Valind and Dr. Eva Kumlien.

Appendix A

Multivariate image data

An image can be created by measuring the intensity distribution in some wavelength band over a spatial area. The image will show samples (pixels) from the distribution describing the measured variable. A sequence of p measurements of the same spatial area creates a multivariate (multitemporal) image data set in which each image represents one variable in a p-dimensional multivariate space. The stack of p images can be described by assigning a p-dimensional vector for each pixel in the two-dimensional image matrix (Fig. A1) The pixel vectors are samples from a multivariate (multitemporal) distribution.

In medial imaging, a multivariate image data set could be a magnetic resonance tomography sequence with images of the same slice using different acquisition parameters [e.g. different repetition times (TR) or echo times (TE)]. A multitemporal image data set could be a PET sequence showing one slice in a dynamic imaging sequence where frames are obtained at different times after the injection of the tracer substance. Alternatively, a multivariate PET sequence could consist of the same slice imaged using different tracer substances. The multivariate and multitemporal data sets can be treated in the same way. A multitemporal distribution is a special case of the multivariate distribution, with time as the only variable. A very high degree of correlation can be expected between image bands in a multitemporal image.

Principal component analysis of multivariate image data

The theory of PCA can be found in many textbooks on multivariate statistics [9–11]. In the area of image analysis, PCA is also known as the Karhunen-Loève transform and as the Hotelling transform [20]. How to apply PCA to image data is clearly demonstrated in [21]. Only a short description will be given here.

The multidimensional image data array with M rows, N columns and p variables (image bands) is unfolded, forming a two-dimensional matrix of size $p(M\,N)$. The sample covariance matrix $\mathbf{S}$ for this data set is of size $p \times p$. A PCA starts with computing the eigenvalues (sorted according to decreasing magnitude) $\hat{\lambda}_{ii}$ and the corresponding (normalized) eigenvectors $\mathbf{u}_i$ of $\mathbf{S}$. These calculations are straightforward using standard algorithms [22]. The

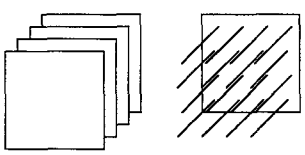

Fig. A 1. A stack of images, i.e. different variables measured for the same scene (slice), can be thought of as an image of pixel vectors. Each pixel vector is then considered to be sample from a multivariate distribution

principal components (PCs) are new variables which point out orthogonal directions with maximum variance in feature space. They are linear combinations, defined by the eigenvectors, of the original variables. All samples are transformed using the eigenvectors, and after the transformation they represent samples from the corresponding PCs.

The transformed samples can be viewed as images when analysing multivariate image data. Calculate the (sorted) eigenvalues and the corresponding (normalized) eigenvectors of **S**. Let the matrix **U** have the eigenvectors as columns. Let the multivariate image be represented as a column vector of images, **I**. Transform **I** to a multivariate image $\mathbf{I}_{PC}$:

$$\mathbf{I}_{PC}=\mathbf{U}'\mathbf{I}. \quad (1)$$

The created image bands, the elements of $\mathbf{I}_{PC}$, are called PC images or score images. The PC image corresponding to the first eigenvector will be termed PC1 and so forth. The transformation defined by **U** is referred to as the PC transformation.

Local PCA

In the description above all pixel vectors in the image were used when calculating the covariance matrix **S**. But in many practical cases it may be desirable to exclude pixel vectors belonging to a static background, for example in a medical image tomograph data set, from the calculations. One way to accomplish this is to use an ROI. After outlining an ROI, let only the pixel vectors which belong to the ROI take part in the calculation of **S**. This is a way to limit the input data set without actually changing the image data. PCA using an ROI is referred to as a local PCA.

Appendix B

Measuring image quality

It is difficult to measure the quality of the PC images obtained through a PCA. In [5] an estimate of the signal-to-noise ratio (SNR) in PC image band i is defined as:

$$\mathrm{SNR}_i = \frac{\lambda_{ii} - \lambda_{pp}}{\lambda_{pp}}, \quad (2)$$

where λ_{ii} is the i:th of p eigenvalues.

This estimate is useful for MR images, which can be assumed to have relatively low noise. The noise properties of PET images are quite different. The background noise is so large that it can be interpreted as signal by the PCA, and the last eigenvalue λ_{pp} will then be a poor estimate of the background noise.

A different method is used in this paper. The SNR is estimated from measurements of variance for each band. The signal in band i is estimated as the variance V within an ROI covering the signalling area, $V_i(\mathrm{ROI}_{\mathrm{signal}})$, for example the skull. The noise in band i is estimated as the variance within an ROI situated in the background, $V_i(\mathrm{ROI}_{\mathrm{noise}})$. Then, the SNR for band i can be estimated using the two measurements:

$$\mathrm{SNR}_i = \frac{V_i(\mathrm{ROI}_{\mathrm{signal}})}{V_i(\mathrm{ROI}_{\mathrm{noise}})}. \quad (3)$$

References

1. Duda R, Hart P. *Pattern classification an scene analysis.* New York: Wiley, 1973.
2. Draper N, Smith H. *Applied regression analysis, 2nd edn.* New York: Wiley, 1981.
3. Harmon H. *Modern factor analysis, 2nd edn.* Chicago: The University of Chicago Press, 1967.
4. Ready P, Wintz P. Information extraction, SNR improvement, and data compression in multispectral imagery, *IEEE Trans Commun* 1973; 21: 1123–1131.
5. Ortendahl D. The application of principal component analysis to mulitvariate MRI data. *Proceedings of the 8th Annual Conference of the Engineering in Medicine and Biology Society* Fort Worth, Texas 1986; 1065–1068.
6. Higer H, Bielke G, eds. *Tissue characterization in MR imaging. Clinical and technical approaches.* Berlin Heidelberg New York: Springer, 1990.
7. Barber D. The use of principal components in the quantitative analysis of gamma camera dynamic studies. *Phys Med Biol* 1980; 25: 283–292.
8. Frouin F, Bazin J-P, Di Paola R. Image sequence processing using factor analysis and compartmental modelling. *SPIE Vol 1137 Science and Engineering of Medical Images* 1989; 37–44.
9. Jackson J. *A user's guide to principal components.* New York: Wiley, 1991.
10. Johnson R, Wichern D. *Applied multivariate statistical analysis, 2nd edn.* Englewoods Cliffs, N.J.: Prentice-Hall, 1988.
11. Jolliffe I. *Principal component analysis.* New York Berlin Heidelberg: Springer, 1986.
12. Barber D, Martel A. Factor analysis revisited. *Eur J Nucl Med* 1992; 19: 467–468.
13. Pedersen F, Bengtsson E, Jonsson D. A numerically derived method for preprocessing of noisy data before applying principal component analysis, *Proceedings of the 8th Scandinavian Conference on Image Analysis.* Norwegian Society for Image Processing and Pattern Recognition, Tromsø 1993; Vol II: 981–988.
14. Pedersen F, Bergström M, Bengtsson E, Maripuu E. Principal component analysis of dynamic PET and gamma camera images: A methodology to visualize the signals in the presence of large noise. *1993 IEEE Conference record Nuclear Science Symposium and Medical Imaging Conference.* San Francisco, Calif. 1993; Vol 3: 1734–1738.
15. Green A, Berman M, Switzer P, Craig M. A transformation for ordering mutispectral data in terms of image quality with implications for noise removal. *IEEE Trans Geosci Remote Sensing* 1988; 26: 65–74.
16. Bengtsson E, Nordin B, Pedersen F. MUSE – a new tool for interactive image analysis and segmentation based on multivariate statistics. *Comput Methods Programs Biomed* 1994; 42: 181–200.
17. Pedersen F. *Interactive explorative analysis of multivariate images using principal components.* PhD thesis, Centre for Image Analysis, Uppsala University, Sweden, 1994.
18. Esbensen K, Geladi P. Strategy of multivariate image analysis (MIA). *Chemometrics and Intelligent Laboratory Systems* 1989; 7: 67–86.
19. Eriksson B, Bergström M, Lilja A, Ahlström H, Långström B, Öberg K. Positron emission tomography (PET) in neuroendocrine gastrointestinal tumors. *Acta Oncol* 1993; 32: 189–196.
20. Gonzalez R, Wintz P. *Digital image processing, 2nd edn.* Reading, Mass.: Addison-Wesley, 1987.
21. Geladi P, Isaksson H, Lindqvist L, Wold S, Esbensen K. Principal component analysis of multivariate images. *Chemometrics and Intelligent Laboratory Systems* 1989; 5: 209–220.
22. Press W, Flannery B, Teukolsky S, Vetterling W. *Numerical recipes in C.* Cambridge: Cambridge University Press, 1988.